energies

MDPI

Article

Techno-Economic Analysis of Intermediate Pyrolysis with Solar Drying: A Chilean Case Study

Tobias Zimmer, Andreas Rudi, Simon Glöser-Chahoud * and Frank Schultmann

Institute for Industrial Production (IIP), Karlsruhe Institute of Technology (KIT), Hertzstr. 16, 76187 Karlsruhe, Germany; tobias.zimmer@kit.edu (T.Z.); andreas.rudi@kit.edu (A.R.); frank.schultmann@kit.edu (F.S.)

* Correspondence: simon.gloeser-chahoud@kit.edu; Tel.: +49-721-608-44592

Abstract: Intermediate pyrolysis can be used to obtain high-quality biofuels from low-value residues such as sewage sludge or digestate. A major obstacle is the high water content of sludgy biomass, which requires an energy-intensive and expensive drying step before pyrolysis. Solar greenhouse drying is an efficient and sustainable alternative to a thermally heated belt dryer. In this study, a techno-economic assessment of intermediate pyrolysis with solar drying is carried out. Marketable products of the process are bio-oil, a substitute for diesel or heating oil, and bio-char with various possible applications. Chile is chosen as the setting of the study as its 4000 km long extension from north to south gives the opportunity to evaluate different locations and levels of solar irradiation. It is found that solar drying results in higher capital investment, but lower fuel costs. Depending on the location and solar irradiation, solar drying can reduce costs by 5–34% compared to belt drying. The break-even price of bio-char is estimated at 300–380 EUR/ton after accounting for the revenue from the liquid bio-oil.

Keywords: intermediate pyrolysis; solar drying; techno-economic assessment; Chile

Citation: Zimmer, T.; Rudi, A.; Glöser-Chahoud, S.; Schultmann, F. Techno-Economic Analysis of Intermediate Pyrolysis with Solar Drying: A Chilean Case Study. *Energies* **2022**, *15*, 2272. https://doi.org/10.3390/en15062272

Academic Editors: Athanasios Rentizelas and Maria Founti

Received: 6 March 2022
Accepted: 16 March 2022
Published: 21 March 2022

1. Introduction

Pyrolysis processes can produce a wide variety of bio-based products and fuels from different biomass resources. Intermediate pyrolysis, with a residence time between 4 and 10 min, is particularly suitable for low-value residues such as sewage sludge, manure, or digestate from biogas plants [1]. Increased utilization of such residues would be advantageous for a number of reasons. First, biomass potentials of lignocellulosic feedstock such as wood are already being exploited on a large scale, while the potential of sludge biomass often remains untapped. In many cases, impurities or hygienic reasons only allow disposal via energy production, meaning there is less competition with other uses of the biomass. Second, sludge biomass is often a very low-cost feedstock, and in some cases, revenue can even be generated from its collection and disposal. However, the processing of sludge biomass is associated with additional technical difficulties, including high water content of the feedstock. Sewage sludge, for instance, contains as little as 10% of solid matter, corresponding to a water content of 90%.

As pyrolysis processes generally require a water content below 15%, sludge feedstock must first be prepared via mechanical and thermal drying. This drying step can involve substantial amounts of process heat and result in significant costs for auxiliary fuels such as natural gas. Moreover, sustainable utilization of biomass resources cannot be based on a major share of heat from fossil sources. As a result, an economic, as well as sustainable, drying process is critical for the utilization of sludge biomass. Solar greenhouse drying has been found to be an efficient and feasible option for different types of sludge, including sewage sludge [2–9], biogas digestate [10,11], and olive oil mill wastes [12,13].

This study analyzes solar drying as part of an intermediate pyrolysis process chain. It is examined whether greenhouse drying is a viable alternative to a thermally heated belt

dryer and how these options for drying affect the economics of producing both high-quality bio-oil and bio-char.

The country of Chile is chosen as the setting for this study for multiple reasons. Due to its enormous extension of more than 4000 km from north to south, Chile covers several zones with different degrees of solar irradiation (Figure 1). In the northern regions, which include parts of the Atacama Desert, some of the highest levels of solar irradiation worldwide can be measured. As a result, solar drying was identified as a promising option for these regions as early as 1984 [14]. Solar potentials in the southern regions, however, are still comparable to those in European countries, where solar drying projects have already been put into practice. Biomass and bioenergy, especially woody biomass, play an important role in the Chilean energy system. Lignocellulosic residues such as cereal straw or forest residues are already utilized to a large extent by biomass combined heat and power plants (CHP) integrated into the forestry industry. Despite the problems with air pollution and deforestation, firewood still accounts for more than 20% of the Chilean primary energy supply.

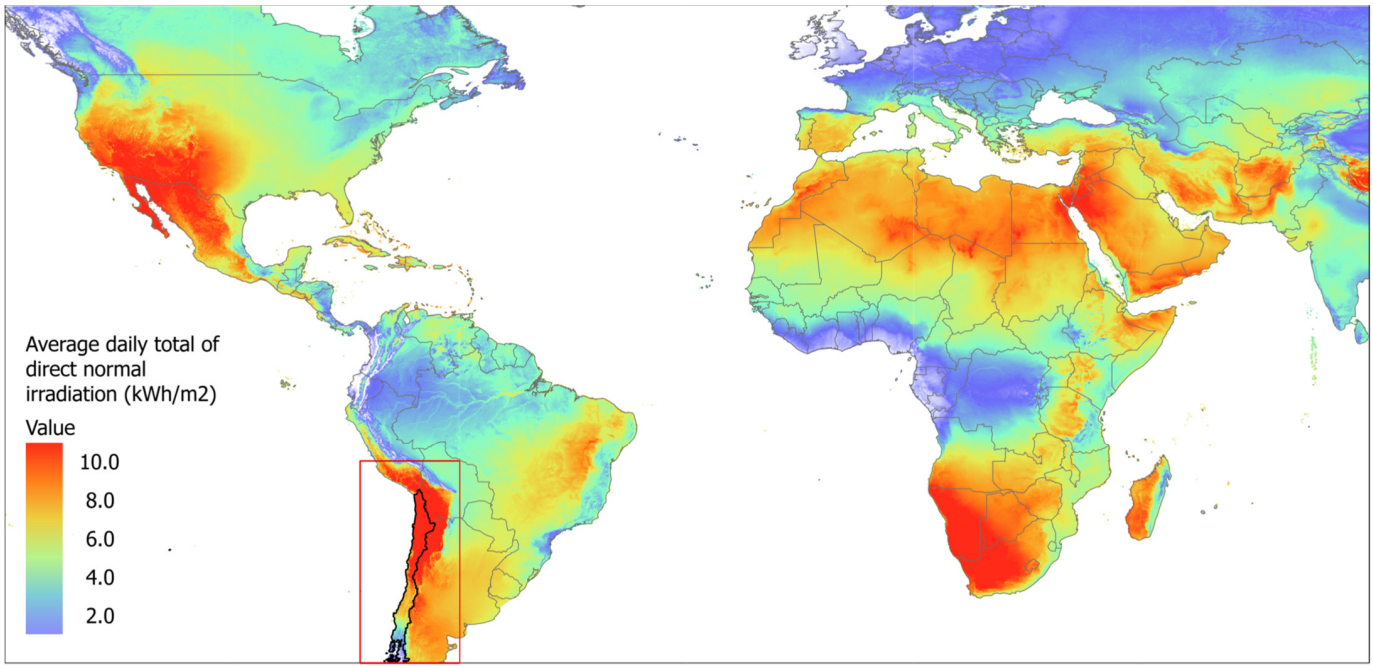

Figure 1. Direct normal irradiation (DNI) in Chile and other countries.

In contrast, sludge biomass is rarely utilized, for instance by single biogas plants. Although various studies have identified a significant energetic potential for biogas production [15,16], very few plants have been built to date. Currently, there are 14 biogas plants with an aggregated capacity of 60 MW, as well as several small plants for self-consumption. Generally, there are almost no fixed feed-in tariffs or subsidies in Chile, so biogas plants, like other bioenergy projects, must be economically viable. Pyrolysis processes offer new options for the economic utilization of sludge by producing higher-value products such as bio-char or upgradable bio-oil instead of power and heat. Where biogas plants can be installed, the digestate, which still contains up to 25% of the energy content, can still be processed via intermediate pyrolysis [17,18].

Despite these benefits, intermediate pyrolysis has not been commercialized at the same scale as other pyrolysis processes such as fast pyrolysis or torrefaction. This may also be due to the fact that intermediate pyrolysis primarily targets challenging and low-value biomass resources. On the other hand, this is precisely what would make the economic implementation of the process a valuable tool for waste management and circular economy. This study explores whether the essential step of feedstock drying can be

decisively improved by solar drying. In the first step, mass and energy balances are calculated for an intermediate pyrolysis plant with either solar or thermal drying. Then, a cost estimation is made to determine the break-even price of bio-char which is required to cover the cost remaining after subtracting the revenue from the bio-oil. Finally, the sensitivity of the results is analyzed with respect to different locations and levels of solar irradiation, plant size, and uncertainty of input parameter values.

2. Background Information

2.1. Intermediate Pyrolysis

During pyrolysis, the thermochemical conversion of organic raw materials is carried out in a high-temperature environment and in the absence of oxygen to prevent combustion. High temperatures (250–600 °C) break the bonds of the molecules, so that long-chain molecules are broken down into short-chain molecules. Pyrolytic decomposition consists of a variety of complex reactions, often involving intermediates that can contribute to further secondary reactions [19]. They require thermal energy and are therefore endothermic reactions. Starting at temperatures of 150 to 220 °C, they are mostly completed at about 500 °C. The result of this decomposition always consists of gaseous, liquid, and solid products. The first two are released from the biomass as gases and vapors and are obtained partly as liquids (pyrolysis oil and water) or as permanent gases (pyrolysis gases) at room temperature. What remains is the pyrolysis char and an ash fraction.

As a result, pyrolysis processes convert the biomass into gaseous, liquid and solid components [20]. The solid product, bio-char, is primarily composed of carbon. The liquid, bio-oil, consists of organic components as well as tars and water. The gas is composed of various components with the most significant ones being carbon dioxide (CO_2), carbon monoxide (CO), hydrogen (H_2), methane (CH_4) and, in small amounts, hydrocarbons (C_nH_m) [21]. This decomposition during a pyrolysis process is also called primary pyrolysis and typically leads to the release of 70% of the volatile components. In the second step, these components react with each other and with the pyrolysis carbon acting as a catalyst in secondary chemical reactions. These reactions are influenced by temperature, residence time and the applied pressure, making it possible to control the composition of the products.

Three types of pyrolysis are often distinguished: slow, intermediate and fast pyrolysis, depending on the process conditions and the process design [22]. Typical process temperatures of intermediate pyrolysis are between slow and fast pyrolysis. As with fast pyrolysis, heating times are also short (up to four seconds). The difference lies in the moderate heating rates and the longer residence times of the feedstock [23], which means that fewer tars can accumulate in the liquid. In addition, the viscosity is lower than that of comparable oils from fast pyrolysis. The liquids produced usually separate into an organic and an aqueous phase. If wood is the feedstock of comparison, intermediate pyrolysis has a liquid fraction of 55% compared to 75% for fast pyrolysis [22]. A comparison of the different pyrolysis processes with respect to the process parameters when using wood as feedstock is shown in Table 1.

Table 1. Classification of pyrolysis processes (woody feedstock) [22].

Process	Temperature [°C]	Heating Rate [°C/s]	Residence Time	Liquid [%]	Solid [%]	Gas [%]
Fast	450–600	100–500	<2 s	75	12	13
Intermediate	400–550	10–100	240–600 s	50 (2 phases)	25	25
Slow	~400	<50	hours	30	35	35

Intermediate pyrolysis is suitable for processing materials with small and large particles and with a moisture content of up to 40%. Waste materials, such as plastics or electronic scrap, and biomasses can be used as feedstock, as long as the carbon content is more than 50% in the dried state of the feed material. Particularly suitable are manure and sewage

sludge due to metallic trace elements that cause the catalytic effect. The process produces none or a very small amount of tar, which can be separated via a spray absorber if necessary.

Bio-char from intermediate pyrolysis is suitable as a long-term fertilizer and soil amendment [24]. It consists mainly of carbon and ash. It can be used as CO_2 storage in the soil, which on the one hand increases the fertility of the soil and on the other hand reduces the emissions of greenhouse gases [22]. As the properties of bio-char can change over time, its stability is of particular interest [25]. To define the stability, the O:C and the H:C ratio can be used. For example, an O:C ratio between 0.2 and 0.6 has a half-life of over 1000 years. In general, the carbon mass fraction of the pyrolysis products can be lowered via a higher temperature [26]. For the quality of the coal, the content of heavy metals and organic pollutants is also important, and certain limits must be observed [21]. In the soil, the coal can act as a nutrient for plant growth and thus lead to a reduction in fertilizer use. In the form of briquettes, bio-char can also be used as a storable fuel and replace fossil coal. Furthermore, the preparation of activated carbon from bio-char is possible. Another option is to use it as feedstock for gasification to obtain a hydrogen-containing gas [22].

The permanent gases from intermediate pyrolysis can be used to produce electricity and heat [27,28] or to undergo further separation and upgrading steps to obtain hydrogen [29] or methanol [30]. Furthermore, the pyrolysis oil has a high calorific value and only a low water content. It is non-polar, so that it can be mixed with vegetable and mineral oils and used directly in engines. This is also due to the low acid number, which prevents corrosion of engine parts [31]. Intermediate pyrolysis has been successfully commercialized by the company PYREG GmbH, which has installed numerous units for the production of bio-char as fertilizer or activated carbon since 2010.

2.2. Solar Drying

Up to now, solar or solar-assisted drying has mainly been used for drying sewage sludge. Due to the similar nature of sewage sludge and digestate, this method of drying is equally suitable for both substrates. In purely solar drying, the water from the substrate to be dried is evaporated by the energy of solar radiation alone. Solar-assisted drying, on the other hand, uses additional energy from other sources to increase the efficiency of the drying process [32]. In this way, the additional energy input can reduce the area required for drying and achieve a consistent drying process throughout the year. The additional heat does not usually have to be generated separately, but can be taken from upstream or downstream processes in the form of waste heat. It can be fed into the drying unit in the form of warm air via the ventilation system or through floor heating systems.

After mechanical dewatering, the feedstock is deposited in greenhouse-like drying halls. Layer thicknesses of 5–35 cm are common for this purpose. In order to maintain uniform digestate moisture over the entire layer thickness and to avoid anaerobic zones, the digestate is regularly turned over by automated or mechanized equipment. Turning frequencies of up to 20 times per day are common [33]. Depending on the turning device, the solar dryer can be operated in batch mode or as a continuous system [34].

In solar-assisted drying, three drying mechanisms occur that evaporate the water in the digestate. These are radiation drying, convection drying and contact drying. In the latter, the sludge is dried by contact with the heated surface of the floor panel. Convection drying is carried out by circulating warm air around the material to be dried. In radiation drying, the electro-magnetic radiation energy of the solar radiation is absorbed and water is evaporated by the resulting increase in temperature. Since pure solar dryers are dependent on the site-specific evaporation capacity of the solar irradiation, their application can be recommended in areas with high evaporation capacity. The evaporation rate in a solar greenhouse dryer is controlled by a range of parameters, including solar irradiation, outdoor temperature, sludge mixing, ventilation and air mixing. Drying rates were modeled as a function of these parameters in [6,7]. A review of different studies on the drying kinetics of sewage sludge in a solar dryer was carried out in [9].

Solar greenhouse drying of sludge has been commercialized by companies such as THERMO-SYSTEM GmbH and HUBER SE. An example of a commercially available solar drying system for sewage sludge is described in [35]. It is worth noting that such projects have been realized not only in exceptionally sunny countries such as Morocco or Spain, but also in Germany and Belgium. Solar greenhouse drying is also a well-established technology for solid, non-sludge biomass such as agricultural products such as fruit, coffee beans and red chili [32,36], or for food processing waste [37].

3. Methods and Data

3.1. Mass and Energy Balances

The process chain begins with the input of the sludge and ends with the storage of bio-oil and bio-char. The downstream transport of the products is not considered, nor is the origin of the feedstock. It is assumed that the pyrolysis plant is directly connected to a biogas plant or sewage treatment plant. A scenario with a central pyrolysis plant supplied by several biogas plants is not considered here, as the transport of sludge biomass is very expensive.

The first step consists of mechanical dewatering. Here, the initial water content is reduced from 90% to 70–65%. The next step is thermal or solar drying, which reduces the water content to 10%. Drying is followed by pyrolysis, in which the biomass is heated to 300–500 °C in the absence of air. During this process, the feedstock decomposes into gas and solid bio-char. The produced gases are fed to a cold trap where the pyrolysis oil and the aqueous solution separate. The permanent gases are burned to cover a part of the energy demand of drying and pyrolysis. The pyrolysis char is separated and cooled down. It is assumed that no waste heat from other processes is available, even though this might be possible in individual cases, for example in connection with a biogas plant. The main steps in the calculation of the mass and energy balances are presented in Figure 2.

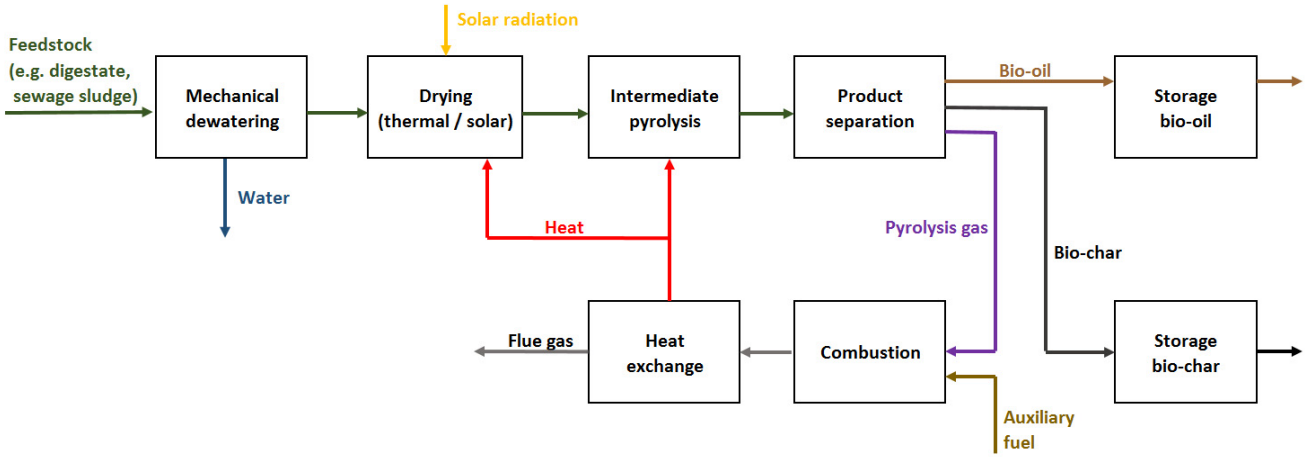

Figure 2. Intermediate pyrolysis process chain.

3.1.1. Dewatering and Drying

Before the biomass can be fed to the pyrolysis process, it must first be dried. For instance, the water content of digestate after fermentation in the digester is about 90%. For pyrolysis to be efficient, the water content must be reduced to 15% [38]. Therefore, the feedstock is mechanically dewatered in the first step. During mechanical dewatering, the solid and liquid fractions are being separated from each other. Equipment such as screw separators, sieve drum filters, centrifugal decanters or vibrating screens are suitable for this purpose. After mechanical dewatering, the water content of the biomass is approximately 70%. To further reduce the water content of the feedstock to the required 15%, thermal or solar drying processes are used. In conventional thermal drying processes, water is removed from the dewatered feedstock via convection by circulating warm air over the material. Systems such as belt dryers, drum dryers, or disk dryers can be used for this

purpose. Drying is an energy-intensive process that has a major influence on the efficiency of the entire plant. For this reason, the heat requirement of the drying process must be taken into account. Here, the heat demand is determined in two steps. First, the energy for heating the biomass to 120 °C is estimated. Then, the energy required to evaporate the corresponding water content is calculated:

$$\dot{Q_{dry}} = \dot{m}_1 \cdot c_{p,1} \cdot \left(\Delta T_{dry}\right)$$

with

$\dot{Q_{dry}}$: heat demand of drying [kJ/s]
$\dot{m}_1$: mass stream of dewatered feedstock [kg/s]
$c_{p,1}$: specific heat capacity of the feedstock $\left[\frac{\text{kJ}}{\text{kg}\cdot\text{K}}\right]$
ΔT_{dry}: temperature difference [K]

To determine the heat requirement for evaporation, the first step is to calculate the mass flow of the water to be evaporated. For the subsequent pyrolysis to run efficiently, a remaining water content of less than 15% is required [22]. Mechanically dewatered sludges have a water content of 70% when they arrive at the drying stage. To determine the mass flow of water to be evaporated, the difference between the input mass flow and the output mass flow is calculated:

$$\dot{m}_{v,\ H20} = w_1 \cdot \dot{m}_3 - w_2 \cdot \frac{DS_{feed} \cdot \dot{m}_1}{1 - w_2}$$

with

$\dot{m}_{v,\ H20}$: mass flow of evaporated water [kg/s]
$\dot{m}_1$: mass flow of feedstock entering pyrolysis [kg/s]
w_1: water content before drying [%]
w_2: water content after drying [%]
DS_{feed}: dry matter [%]

3.1.2. Belt Drying

Digestate or sewage sludge can be thermally dried using a belt dryer. In this study, the two-belt dryer with extrusion described in [39] serves as the basis for the drying step. Further information and illustrations of this commercially available sludge dryer can be found in [40]. This two-belt dryer has the advantage over a single-belt dryer that a smaller area is required and that the dry material is turned and broken up, which results in new surfaces and more efficient drying. The extruder distributes the dry material evenly on the belt and creates breaking points and good ventilation.

The equipment cost of the dryer area can be estimated as a function of the total belt area. To calculate the belt area, parameters are taken from [39], where further information about the kinetics and optimal control of a belt dryer can be found. The sludge dryer operates at 120 °C, has a drying time of 2 to 2.5 h, and the bed height is 5 to 10 cm. The heat requirement is 0.8 to 0.85 kWh per kg of evaporated water. With these values, the following equation can be used to calculate the belt area.

$$A_{belt} = \frac{\dot{m}_2 \cdot t_{dry}}{\rho_{feed} \cdot h_{dry}}$$

A_{belt}: belt area [m^2]
$\dot{m}_2$: mass flow of dewatered feedstock [kg/s]
t_{dry}: drying time [s]
ρ_{feed}: density of dewatered feedstock [kg/m^3]
h_{dry}: bulk height [m]

3.1.3. Solar Drying

The base area is the main parameter required to estimate the cost of a solar greenhouse dryer at location *i*. It can be calculated based on the evaporation rate [5]:

$$A_{greenhouse} = \frac{\dot{m}_{e,i}}{e_{v,i}}$$

$$\dot{m}_{e,i} = \dot{m}_{s,i}\left(1 - \frac{DS_{i,i}}{DS_{m,i}}\right)$$

$A_{greenhouse}$: base area of greenhouse dryer [m^2]
$\dot{m}_{e,i}$: water to be evaporated [m^3/h]
$e_{v,i}$: average evaporation rate at location *i* [kg/m^2-h]
$\dot{m}_{s,i}$: loading rate of wet feedstock [m^3/h]
$DS_{i,i}$: initial dry solids content of the feedstock [kg solids/kg sludge]
$DS_{m,i}$: target dry solids content of the feedstock [kg solids/kg sludge]

The evaporation rate is estimated with the following equation provided in [7]:

$$e_{v,i} = (\rho K_v\ 1.964{\cdot}10^{-11})[(R_{0,i} + 1100)^{2.322}(T_{0,i} + 13)^{1.292}(K_v)^{-0.577} \cdot(K_m + 0.0001)^{0.013}(DS_{i,i} + 0.26)^{-0.353}]$$

ρ: air density (1.13 kg/m^3)
K_v: ventilation rate [m^3/m^2-h]
$R_{0,i}$: solar irradiation at location *i* [W/m^2]
$T_{0,i}$: ambient air temperature at location *i* [°C]
K_m: air mixing rate [m^3/m^2-h]
$DS_{i,i}$: initial dry solids content of the feedstock [kg solids/kg sludge]

3.1.4. Pyrolysis

After drying, the feedstock enters the main process, the intermediate pyrolysis. Thermo-catalytic reforming, in which a reforming step takes place after pyrolysis, is used as a reference process for intermediate pyrolysis due to its enhanced product properties [41,42]. The input mass flow of the pyrolysis corresponds to the output mass flow of the drying process. However, it is necessary to determine how the input material flow is split up into the individual product flows during pyrolysis. Mass and energy yields of the pyrolysis products were adopted from [31], where reaction mechanisms, as well as the ultimate analysis of feedstock and products, are described in detail. Depending on the process parameters, the composition, as well as the quantities of the products differ (Table 2). The ash fraction is added to the charcoal fraction, as the ash is only released when the charcoal is burned.

Table 2. Product yields of the TCR® process (biogas digestate) [31].

Scenario	A	B	C
Temperature pyrolysis [°C]	450	450	450
Temperature reforming [°C]	-	450	750
Fraction pyrolysis gas [vol%]	18	20	36
Fraction pyrolysis oil [wt%]	12	13	4
Fraction water phase [wt%]	30	29	25.9
Fraction bio-char including ash [wt%]	40	38	34.1
Heating value pyrolysis gas [MJ/m^3]	9.7	13.1	14.4
Heating value bio-oil [MJ/kg]	34.1	36.3	35.4
Heating value bio-char [MJ/kg]	16.7	18.9	17.3

For the techno-economic modeling of the reactor, the pyrolysis unit for domestic organic waste described in [43] is used as a basis. In its design, the Auger reactor with the twin-screw used there is similar to the TCR® coaxial screw reactor. In both, the principle of recirculating char as a catalyst within the reactor is applied. For the reformer, a continuously operated kettle reactor is used. According to [44], volume is the characteristic parameter for kettle reactors. With the following equation, the volume can be derived from the mass flow and other parameters:

$$V_{ref} = \frac{\dot{m}_3}{\rho_{char}} \cdot t_{ref} \cdot \frac{100}{\phi_{ref}}$$

with

V_{ref}: required volume of reformer [m^3]
$\dot{m}_3$: mass flow of feedstock to pyrolysis [kg/s]
ρ_{char}: density bio-coal [kg/m^3]
t_{ref}: average throughput time [s]
ϕ_{ref}: average fill rate of reformer [%]

The average throughput time of the reforming is based on the average throughput time of the preceding pyrolysis with 5 min [38]. The average filling rate is set to 20% as the pyrolysis charcoal needs contact with the gases for the pyrolysis products to interact [17].

Several heat exchangers are required to supply the plant with heat as needed. Two heat exchangers are operated with hot flue gas, while the condenser, which cools and partially condenses the gaseous pyrolysis products, is supplied with cold water. This depends on the prevailing process conditions. For the selection of suitable heat exchangers, [44] is used as a reference, as they provide a list of heat exchanger systems with their areas of application and parameters. Welded plate heat exchangers are suitable for use with flue gas, as they can be operated in high temperature ranges of more than 400 °C. According to [44], shell-and-tube exchangers are recommended as condensers when direct heat transfer is not desired. The heat transfer area is used as a characteristic parameter for heat transfer. To calculate it, the average logarithmic temperature difference is determined first:

$$\Delta T_{log} = \frac{\Delta T_1 - \Delta T_2}{\ln\left(\frac{\Delta T_1}{\Delta T_2}\right)}$$

with ΔT_1 denoting the larger temperature difference and ΔT_2 the smaller temperature difference at the ends of the heat exchanger. The temperature is measured between the inlet of one medium and the outlet of the other medium, as the heat exchangers operate according to the countercurrent principle. The heat transfer area can then be calculated as follows:

$$A_{heat} = \frac{Q_x}{\Delta T_{log} \cdot u}$$

A_{heat}: heat transfer area of the heat exchanger [m^2]
Q_x: heat demand [W]
ΔT_{log}: mean logarithmic temperature difference [K]
u: heat transfer coefficient of the heat exchanger [W/m^2K]

For the heat transfer coefficients, values of 80 W/m^2K for the plate heat exchangers and 1500 W/m^2K for the condenser are taken from [44].

4. Economic Evaluation

For the economic evaluation, [44] is used as a reference, as cost functions for most standard equipment are provided there. Some cost functions are taken from other sources: The cost of the pyrolysis reactor is based on the cost of the Auger reactor in [43]. For the dryer, the cost function in [45] is used. The cost of the decanter for mechanical dewatering is based on [46]. For solar greenhouse drying, a price of 300 EUR/m^2 is assumed [5]. The

capital requirement is determined by estimating the acquisition cost of the main equipment through cost functions and adjusting it to current prices using a price index. Finally, the total capital requirement is estimated using surcharge factors expressed as a percentage of the cost of the equipment. The dimensioning of the equipment also has a significant impact on the purchase price. Economies of scale describe the phenomenon that acquisition costs increase disproportionately when capacity is increased, which can be represented by the following exponential function [47]:

$$C = C_{base} \cdot \left(\frac{Capa}{Capa_{base}} \right)^{R}$$

with

C: cost of equipment
C_{base}: cost of equipment with base capacity
$Capa$: capacity of equipment
$Capa_{base}$: base capacity of equipment
R: scaling factor

The cost of capital includes the financing and depreciation of the assets. An annuity method is used to calculate the annual cost of capital [48]:

$$A = K_0 \cdot \frac{(1+i)^n \cdot i}{(1+i)^n - 1}$$

with

A: annuity
K_0: capital value at time 0
i: interest rate
n: depreciation time

Linear depreciation of the acquisition costs is applied over the entire utilization period, for which a value of 20 years is assumed. The interest rate consists of a base interest rate of 10% and a country-specific risk premium. The risk premium assesses uncertainties such as political instability or currency developments [49]. For Chile, a risk premium of 0.98% is estimated in [50].

Intermediate pyrolysis produces two valuable products, liquid bio-oil and solid bio-char. An advantage of bio-oil produced by the intermediate pyrolysis process is that it has a lower tar content and can be used directly for thermal heat generation [51]. The oil from the TCR process could even be mixed directly with diesel and used in vehicles [52]. Although Chile has laws that allow biofuel blending, market introduction and distribution would be excessively demanding for a single biofuel project. Therefore, it was assumed that the bio-oil would be used as a heating oil substitute and could be sold at the price of fuel oil.

The revenue from the sale of the bio-char is more difficult to quantify, as it can be used not only as a fuel, but also for other potentially more profitable applications, such as soil improvement. Because of this uncertainty, only the minimum price of the bio-char is determined with a break-even calculation. For this purpose, the revenues from the sale of bio-oil are subtracted from the total annual costs of the plant and divided by the annual production of bio-char.

$$price_{char} = \frac{cost_{total} - revenue_{oil}}{output_{char}}$$

5. Results and Discussion

5.1. Base Case (Concepción, Region VIII)

In the first step of the economic evaluation, solar drying and belt drying are compared with regard to the price of bio-char and the cost structure of the plant. For this base case, the city of Concepción in the eighth region (Bío-Bío) is selected as a plant location as it

combines attractive levels of solar irradiation with a variety of potential biomass resources from waste management, forestry, or agriculture. Other locations with higher or lower solar potentials are explored in the next section. A production of 3577 tons of bio-char per year as well as the use of natural gas as auxiliary fuel is assumed in the base case.

The minimum price for bio-char as well as the costs per ton are shown in Table 3. It can be seen that solar drying results in higher capital costs due to the more expensive greenhouse system (see Table 4), but lower fuel and overall costs. It was assumed that bio-oil, the liquid pyrolysis product, was used as a substitute for fuel oil. Although significantly less oil is produced than coal, the economic value has a significant impact on the break-even calculation.

Table 3. Break-even price in EUR of bio-char (base case with 3577 tons bio-char per year).

	Configuration with Greenhouse Solar Drying	**Configuration with Belt Dryer (Natural Gas)**
Capital (EUR/year)	1,078,740	879,692
Labor (EUR/year)	350,749	350,749
Fuels (EUR/year)	363,111	798,913
Revenue bio-oil (EUR/year)	−578,240	−575,835
Total cost (EUR/year)	1,214,359	1,446,744
Bio-char produced (ton/year)	3577	3577
Break-even price bio-char	339.5	404.5

Table 4. Installed equipment cost in EUR (base case with 3577 tons bio-char per year).

Equipment	**Configuration with Greenhouse Solar Drying**	**Configuration with Belt Dryer (Natural Gas)**
Storage feedstock	79,496	
Decanter	46,397	
Dryer	1,566,544	760,971
Pyrolysis reactor	2,029,668	
Reformer	75,436	
Condenser	2301	
Heat supply	32,897	103,935
Flue gas cleaning	6591	
Ammonia scrubber	10,493	
Storage bio-coal	87,609	
Storage bio-oil	43,691	
Total	3,981,124	3,246,532

5.2. Regional Analysis

Due to the enormous geographical extension from north to south, the level of solar irradiation differs very significantly between Chilean regions (Figure 3). In general, solar irradiation decreases from north to south, while the diversity and quantity of biomass resources increase due to stronger agricultural activity. However, it can be assumed that a sufficient amount of sludge biomass can be found in all regions due to the flexibility of the intermediate pyrolysis process. Examples of feedstock that can be found in Chile and that has been successfully treated via intermediate pyrolysis are paper sludge [41,53], grape pomace [54], red algae [55], chicken manure [56] and digestate [10,31]. The city of Concepción was selected for the base case because the eighth region combines a variety of potential organic sludge feedstocks with high solar potential. To explore how different levels of solar irradiation affect the cost of bio-char, the analysis was conducted for different exemplary cities in Chile. Results are shown in Table 5. It can be seen that solar greenhouse drying is competitive with thermal drying based on natural gas in all regions. In the southern cities from Chillan to Puerto Montt, thermal drying with wood chips results in lower costs per ton of bio-char. However, it must be pointed out that the availability of cheap wood chips is limited to certain southern regions with a high degree of commercial forestry.

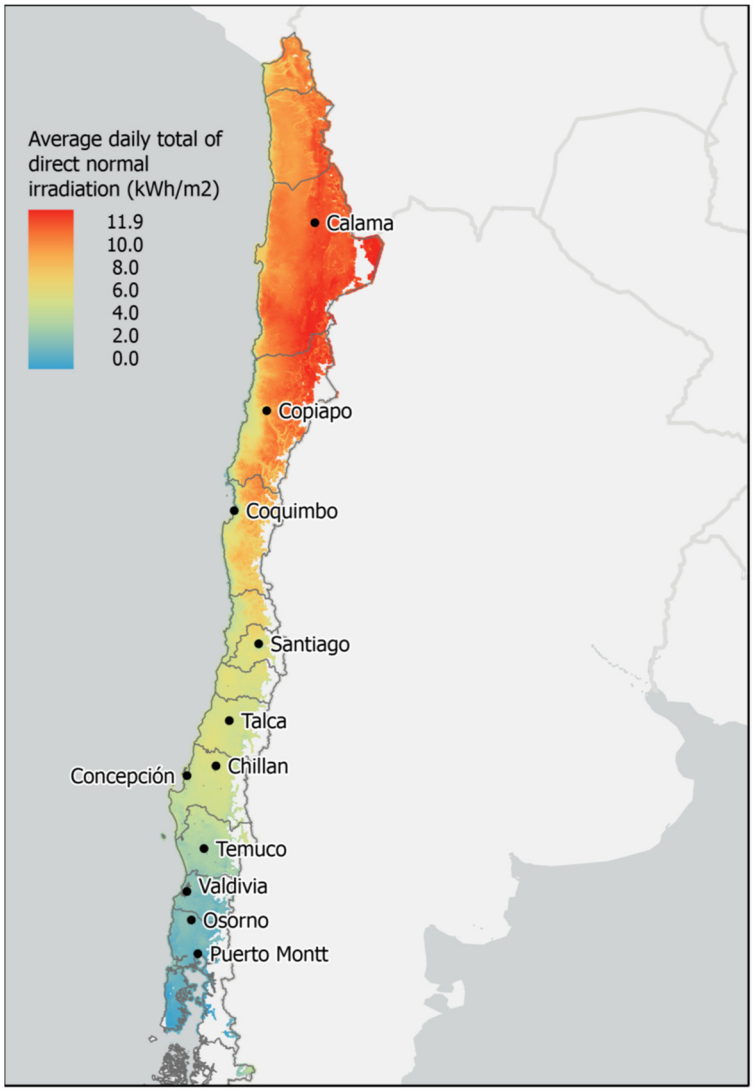

Figure 3. Locations and levels of solar irradiation.

Table 5. Regional analysis of solar drying performance and bio-char price.

Location	Annual Average Solar Irradiation (W/m^2)	Standard Deviation Solar Irradiation (%)	Area Solar Dryer (m^2)	Break Even Price Bio-Char (EUR/ton)
Calama	331.92	1.1	4484	300.50
Copiapo	292.82	2.4	4333	297.19
Coquimbo	227.99	2.7	5909	331.72
Santiago	242.45	5.4	4988	311.54
Talca	225.95	5.0	5546	323.76
Chillan	227.05	4.0	5822	329.82
Concepción	222.90	3.4	6266	339.54
Temuco	189.82	5.7	7110	358.03
Valdivia	182.01	5.8	7190	359.78
Osorno	170.01	6.1	7696	370.86
Puerto Montt	153.22	6.4	8413	386.58
	Belt dryer with natural gas (7.55 EUR/GJ)			404.5
	Belt dryer with wood chips (3.74 EUR/GJ)			325.1

5.3. Economies of Scale

In the techno-economic evaluation, it was assumed that the equipment costs are subject to economies of scale, in other words, that larger plants can achieve lower costs per ton. However, it should not be assumed that capacity and throughput can be arbitrarily high. On the one hand, sludge biomass can only be transported with considerable expense due to its high water content. In a realistic scenario, the pyrolysis plant would be located in the immediate vicinity or directly on the premises of the plant providing the feedstock, for instance, a wastewater treatment plant. The capacity of the pyrolysis plant would therefore be limited to feedstock created by this facility. On the other hand, very large plant sizes can only be realized in Chile in the metropolitan regions of Santiago, Valparaíso, or Concepción. In more remote and rural areas, for instance, in the very northern or southern regions, smaller plant sizes and more decentralized concepts would be more suitable.

The economies of scale for the base case in the eighth region are shown in Figure 4. Significant cost reductions are achieved starting from 2000 tons of bio-char produced per year. With a water content of 90%, this corresponds to 45,000 tons of sludge feedstock per year. This value falls within the range of commercial greenhouse dryers, with single plants now capable of processing more than 150,000 tons of sludge per year.

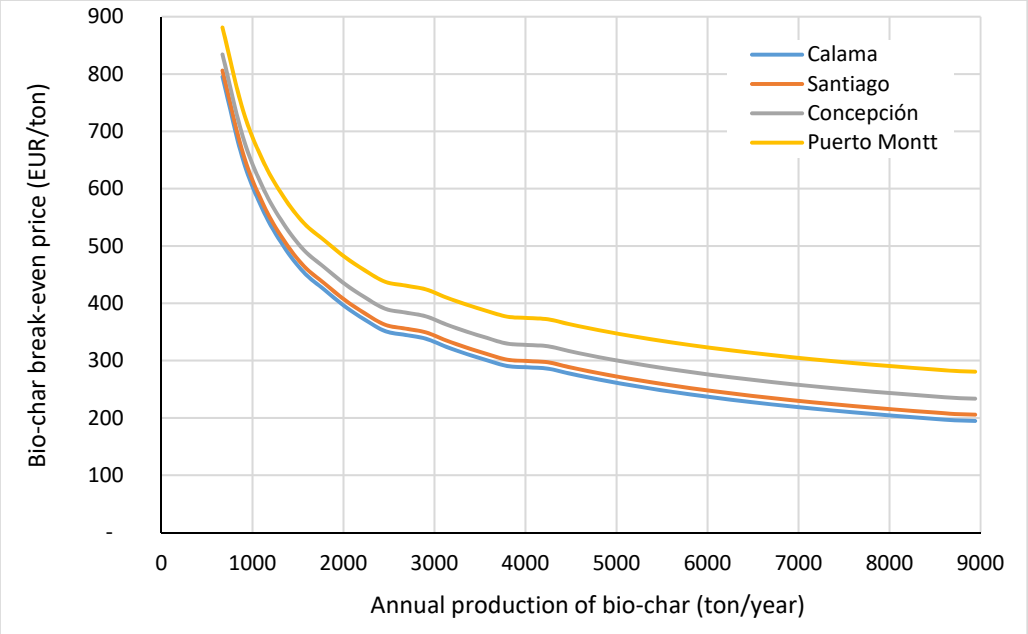

Figure 4. Economies of scale of bio-char production via pyrolysis in the Bío-Bío region.

5.4. Monte Carlo Simulation

The described model and the presented results are based on several input parameters which are subject to uncertainty. The impact of these uncertainties can be investigated through a Monte Carlo simulation, which is a numerical method based on the law of large numbers. It has a wide range of applications in different scientific disciplines, which in includes the evaluation of economic risks. First, relevant parameters are identified and assigned an interval of variation or a distribution function. Random values are then drawn from these intervals, and the model is run with these values. The process of calculating the model is repeated so often that the mean value can approach the expected value, for example, 10,000 times. The results of the individual repetitions are used to calculate the arithmetic mean together with the standard deviation.

Relevant parameters are those that have a major influence on the process and are subject to external influences. Table 6 provides an overview of these parameters. The deviation of the annual solar irradiation was based on historic data from a Chilean geographical information system for solar potentials [57]. Scenarios for the price of natural gas and

heating oil are based on the Annual Energy Outlook [58]. As a result, gas and oil price are not independent, but correspond to a single scenario randomly chosen in each iteration of the simulation.

Table 6. Parameter ranges for Monte Carlo simulation.

Parameter	Minimum	Default	Maximum
Water content after decanter (%)	65	70	75
Belt dryer efficiency (%)	65	70	75
Burner efficiency (%)	85	90	95
Solar irradiation	Location-dependent, see mean and standard deviation in Table 5		
Interest rate (%)	7.5	10	12.5
Depreciation period (years)	15	20	25
Operating hours (h/a)	5250	7000	8750
Natural gas price (EUR/GJ)	7.55	7.55	13.71
Wood chips price (EUR/t)	30.18	37.43	44.67
Pyrolysis oil price (EUR/t)	466.82	778.03	1089.24
Electricity price (EUR/kWh)	0.08	0.14	0.20

The results of a Monte Carlo simulation with 10,000 iterations are shown for a solar drying and thermal drying configuration in Figure 5. Parameter values were drawn equally distributed from the range between minimum and maximum. It can be observed that the average bio-char break-even price overall simulation runs is lower for solar drying (275.51 EUR/ton) than for thermal drying (383.17 EUR/ton). However, it can also be seen that the values for solar drying show a greater spread, which is also reflected by the standard deviation of 37% of the mean value. In contrast, the standard deviation is 27% of the mean for the thermal drying configuration. This is because the solar greenhouse dryer is more expensive than the belt dryer and the techno-economic evaluation is very sensitive to all driving factors of the capital cost, such as the interest rate or the depreciation period. It must be pointed out that this uncertainty reflects less the risks of the project rather than the accuracy of the assessment. A preliminary, order-of-magnitude estimate such as this necessarily relies on different assumptions, for instance with regard to the interest rate or overhead costs. However, if the project was implemented, these uncertainties would diminish with each planning phase up to the point of operation. However, after the start-up of the plant, the actual operating hours per year and the fuel costs are decisive. Here, solar drying has the advantage that the annual solar radiation hardly varies, while the price of natural gas as well as wood chips is subject to considerable uncertainty.

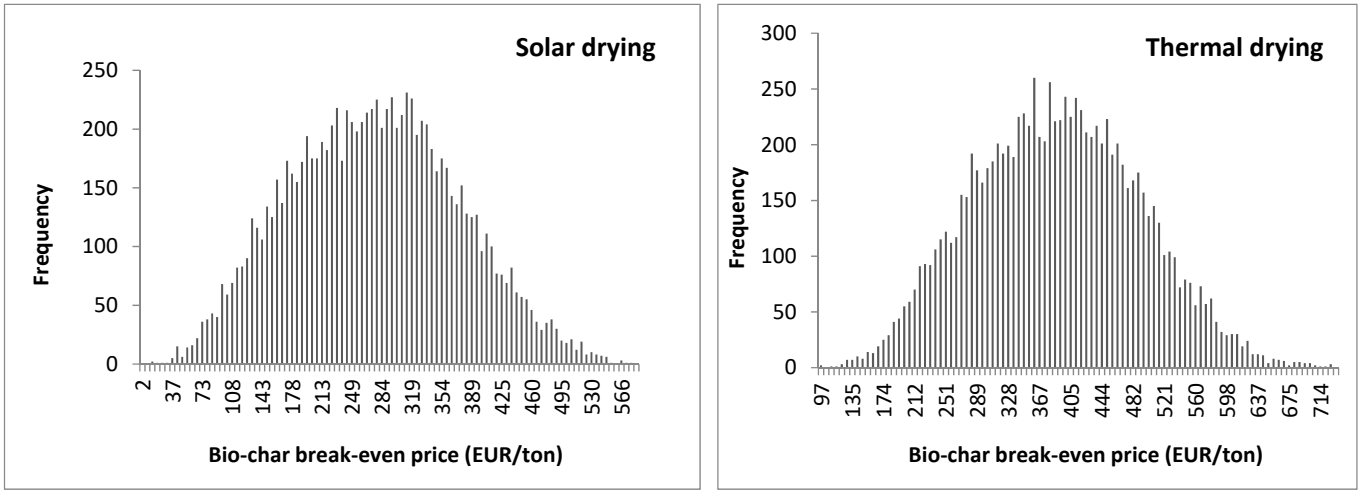

Figure 5. Results of Monte Carlo simulation for solar drying (**left**) and thermal drying (**right**) configuration.

The mean values produced by the Monte Carlo simulation do not exactly match the values of the base case, which can be attributed to the prices for fossil fuels. Oil and gas

prices in the base case correspond to the reference case of the eia Annual Energy Outlook, while the simulation randomly draws from all scenarios. Very low values of as little as 50 EUR per ton of bio-char result from a high oil price scenario where substantial revenue can be achieved with the bio-oil alone.

6. Summary and Outlook

Pyrolysis can be used to obtain high-value products such as bio-char from sludge biomass. A technical and economic obstacle is the high water content of the sludge, which requires energy-intensive drying. In this article, solar greenhouse drying was evaluated as an alternative to belt drying in a pyrolysis system. A techno-economic assessment was carried out to estimate the break-even-price of bio-char and to explore the impact of different parameters such as plant capacity and location. The country of Chile was chosen as the setting of the study as it features different levels of solar irradiation as well as a wide range of biomass resources due to its north-south extension.

It was found that solar drying is an economical alternative to belt drying with natural gas in all regions of Chile, but especially in the northern regions with extreme solar radiation. With solar drying, bio-char prices between 300 and 387 EUR/ton can be achieved, depending on the chosen plant location. In comparison, the bio-char price was estimated to be between 359 and 484 EUR/ton in [56]. The estimated bio-char break-even price could allow an economically feasible application for soil improvement, activated carbon, or as feed additive [24]. However, the price of bio-char is too high to use as a fuel, for instance for co-firing in coal-fired power plants. In the more southern regions with a high degree of forestry, wood chips are an inexpensive alternative to natural gas. With a price of less than 40 EUR/ton of wood chips, thermal drying leads to a 5–10% lower bio-char price than solar drying. The results indicate that solar drying can be beneficial in all regions of Chile and would not be limited to the northern regions. As the southern locations considered in this article (Valdivia, Osorno, Puerto Montt) are similar to European countries such as France, Germany or Austria, the concept could be transferable to a wide range of locations.

One way to increase the economics of the concept would be to upgrade the bio-oil. Intermediate pyrolysis produces an oil that can be treated via hydrodeoxygenation, emulsification, hydrocracking or catalytic esterification to obtain transportation fuel [28,38]. Moreover, it is possible to extract valuable chemicals from the organic phase which could be used as flavoring additives or preservatives [52]. It was assumed that the feedstock—digestate, sewage sludge—could be obtained at no cost. In a waste management scenario, where a premium would be paid for disposing of the sludge, the economic viability could be better. Conversely, if there would be a market price, for instance for digestate as a fertilizer, the break-even price of the char would be higher.

With regard to the excellent solar potentials in Chile, exploring solar thermal energy in combination with a thermo-chemical process such as pyrolysis could also be promising. Solar thermal energy, for instance, generated with tube collectors, could not only support a conventional drying process, but also provide process heat for pyrolysis or subsequent conversion and upgrading processes. For instance, solar thermal drying with a parabolic trough solar collector was investigated in [59]. The feedstock was olive mill sludge, which is also produced in Chile and which could be processed via intermediate pyrolysis. Compared to solar greenhouse drying, however, there have been few studies or example projects to date that could serve as a basis for techno-economic evaluation.

Author Contributions: Conceptualization, T.Z. and S.G.-C.; methodology, T.Z. and A.R.; writing—original draft preparation, T.Z.; writing—review and editing, T.Z., A.R., S.G.-C. and F.S.; visualization, T.Z.; supervision, S.G.-C. and F.S.; project administration, S.G.-C. and F.S.; funding acquisition, S.G.-C. and F.S. All authors have read and agreed to the published version of the manuscript.

Funding: This research was funded by the German Federal Ministry of Education and Research (BMBF), grant number 031B0056A (SeMoBioEnergy).

Institutional Review Board Statement: Not applicable.

Informed Consent Statement: Not applicable.

Acknowledgments: We acknowledge support by the KIT-Publication Fund of the Karlsruhe Institute of Technology.

Conflicts of Interest: The authors declare no conflict of interest.

References

1. Kazawadi, D.; Ntalikwa, J.; Kombe, G. A Review of Intermediate Pyrolysis as a Technology of Biomass Conversion for Coproduction of Biooil and Adsorption Biochar. *J. Renew. Energy* **2021**, *2021*, 5533780. [CrossRef]
2. Đurđević, D.; Blecich, P.; Jurić, Ž. Energy Recovery from Sewage Sludge: The Case Study of Croatia. *Energies* **2019**, *12*, 1927. [CrossRef]
3. Di Fraia, S.; Figaj, R.D.; Massarotti, N.; Vanoli, L. An integrated system for sewage sludge drying through solar energy and a combined heat and power unit fuelled by biogas. *Energy Convers. Manag.* **2018**, *171*, 587–603. [CrossRef]
4. Garanto, O. Solar Sludge Drying Technology and Dried Sludge as Renewable Energy—Closing the Loop. *J. Traffic Transp. Eng.* **2016**, *4*, 4. [CrossRef]
5. Kurt, M.; Aksoy, A.; Sanin, F.D. Evaluation of solar sludge drying alternatives by costs and area requirements. *Water Res.* **2015**, *82*, 47–57. [CrossRef]
6. Seginer, I.; Bux, M. Modeling Solar Drying Rate of Wastewater Sludge. *Dry. Technol.* **2006**, *24*, 1353–1363. [CrossRef]
7. Seginer, I.; Ioslovich, I.; Bux, M. Optimal control of solar sludge dryers. *Dry. Technol.* **2007**, *25*, 401–415. [CrossRef]
8. Youssef, A.S.; Kahil, M.A. Solar Sludge Drying for Medina Al-Munawarah Sewage Treatment Plant in the Kingdom of Saudi Arabia. *J. Environ. Eng.* **2016**, *142*, 5016006. [CrossRef]
9. Bennamoun, L. Solar drying of wastewater sludge: A review. *Renew. Sustain. Energy Rev.* **2012**, *16*, 1061–1073. [CrossRef]
10. Maurer, C.; Müller, J. Drying Characteristics of Biogas Digestate in a Hybrid Waste-Heat/Solar Dryer. *Energies* **2019**, *12*, 1294. [CrossRef]
11. Rehl, T.; Müller, J. Life cycle assessment of biogas digestate processing technologies. *Resour. Conserv. Recycl.* **2011**, *56*, 92–104. [CrossRef]
12. Montero, I.; Miranda, M.; Sepúlveda, F.; Arranz, J.; Rojas, C.; Nogales, S. Solar Dryer Application for Olive Oil Mill Wastes. *Energies* **2015**, *8*, 14049–14063. [CrossRef]
13. Maragkaki, A.; Galliou, F.; Markakis, N.; Sabathianakis, G.; Tsompanidis, C.; Lolos, G.; Mavrogiannis, G.; Koukakis, G.; Lasaridi, K.; Manios, T. Initial Investigation of the Solar Drying Method for the Drying of Olive Oil By-Products. *Waste Biomass Valorization* **2016**, *7*, 819–830. [CrossRef]
14. Román, R. Solar drying in northern Chile. *Sol. Wind Technol.* **1984**, *1*, 49–58. [CrossRef]
15. Bidart, C.; Fröhling, M.; Schultmann, F. Livestock manure and crop residue for energy generation: Macro-assessment at a national scale. *Renew. Sustain. Energy Rev.* **2014**, *38*, 537–550. [CrossRef]
16. Chamy, R.; Vivanco, E. *Potencial de Biogás. Identificación y Clasificación de los Distintos Tipos de Biomasa Disponibles en Chile para la Generación de Biogás*; Instituto Forestal: Santiago, Chile, 2007.
17. Hornung, A.; Binder, S.; Neumann, J.; Apfelbacher, A. *Biobattery: Integrated Heat and Power from Biomass Residues as a Contribution to the European Energy Transition*; Fraunhofer: Vienna, Austria, 2015.
18. Feng, Q.; Lin, Y. Integrated processes of anaerobic digestion and pyrolysis for higher bioenergy recovery from lignocellulosic biomass: A brief review. *Renew. Sustain. Energy Rev.* **2017**, *77*, 1272–1287. [CrossRef]
19. Kaltschmitt, M.; Hartmann, H.; Hofbauer, H. *Energie aus Biomasse*; Springer: Berlin/Heidelberg, Germany, 2016; ISBN 978-3-662-47437-2.
20. McKendry, P. Energy production from biomass (part 2): Conversion technologies. *Bioresour. Technol.* **2002**, *83*, 47–54. [CrossRef]
21. Schmitt, N.; Apfelbacher, A.; Jäger, N.; Daschner, R.; Stenzel, F.; Hornung, A. Thermo-chemical conversion of biomass and upgrading to biofuel: The Thermo-Catalytic Reforming process—A review. *Biofuels Bioprod. Bioref.* **2019**, *158*, 3. [CrossRef]
22. Hornung, A. *Transformation of Biomass: Theory to Practice*; Wiley: Hoboken, NJ, USA, 2014; ISBN 9781119973270.
23. Yang, Y.; Brammer, J.G.; Mahmood, A.S.N.; Hornung, A. Intermediate pyrolysis of biomass energy pellets for producing sustainable liquid, gaseous and solid fuels. *Bioresour. Technol.* **2014**, *169*, 794–799. [CrossRef] [PubMed]
24. Hornung, A.; Stenzel, F.; Grunwald, J. Biochar—Just a black matter is not enough. *Biomass Conv. Bioref.* **2021**. [CrossRef]
25. Enders, A.; Hanley, K.; Whitman, T.; Joseph, S.; Lehmann, J. Characterization of biochars to evaluate recalcitrance and agronomic performance. *Bioresour. Technol.* **2012**, *114*, 644–653. [CrossRef] [PubMed]
26. Crombie, K.; Mašek, O.; Sohi, S.P.; Brownsort, P.; Cross, A. The effect of pyrolysis conditions on biochar stability as determined by three methods. *GCB Bioenergy* **2013**, *5*, 122–131. [CrossRef]
27. Yang, Y.; Brammer, J.G.; Wright, D.G.; Scott, J.A.; Serrano, C.; Bridgwater, A.V. Combined heat and power from the intermediate pyrolysis of biomass materials: Performance, economics and environmental impact. *Appl. Energy* **2017**, *191*, 639–652. [CrossRef]
28. Boscagli, C.; Tomasi Morgano, M.; Raffelt, K.; Leibold, H.; Grunwaldt, J.-D. Influence of feedstock, catalyst, pyrolysis and hydrotreatment temperature on the composition of upgraded oils from intermediate pyrolysis. *Biomass Bioenergy* **2018**, *116*, 236–248. [CrossRef]
29. Sofia, D.; Giuliano, A.; Poletto, M.; Barletta, D. Techno-economic analysis of power and hydrogen co-production by an IGCC plant with CO_2 capture based on membrane technology. In Proceedings of the 12th International Symposium on Process Systems Engineering and 25th European Symposium on Computer Aided Process Engineering, Copenhagen, Denmark, 31 May–4 June 2015; Elsevier: Amsterdam, The Netherlands, 2015; pp. 1373–1378, ISBN 9780444634290.

30. Giuliano, A.; Freda, C.; Catizzone, E. Techno-Economic Assessment of Bio-Syngas Production for Methanol Synthesis: A Focus on the Water-Gas Shift and Carbon Capture Sections. *Bioengineering* **2020**, *7*, 70. [CrossRef]
31. Neumann, J.; Meyer, J.; Ouadi, M.; Apfelbacher, A.; Binder, S.; Hornung, A. The conversion of anaerobic digestion waste into biofuels via a novel Thermo-Catalytic Reforming process. *Waste Manag.* **2016**, *47*, 141–148. [CrossRef]
32. Kumar, M.; Sansaniwal, S.K.; Khatak, P. Progress in solar dryers for drying various commodities. *Renew. Sustain. Energy Rev.* **2016**, *55*, 346–360. [CrossRef]
33. Bux, M. Bauarten solarer Klärschlammtrocknungsanlagen. *Energ. Aus.* 2013. Available online: https://www.vivis.de/wp-content/uploads/EaA10/2013_EaA_949_960_Bux.pdf (accessed on 5 March 2022).
34. Jacobs, U. Kosten und Wirtschaftlichkeit der Klärschlammtrocknung. *Energ. Abfall* **2013**, *10*, 961–974.
35. HUBER SE. HUBER Sludge Turner SOLSTICE®Solar Sewage Sludge Drying. Available online: https://www.huber.de/fileadmin/01_products/04_sludge/04_trocknen/01_srt/pro_solstice_en.pdf (accessed on 5 March 2022).
36. Mathew, A.A.; Venugopal, T. Solar power drying system: A comprehensive assessment on types, trends, performance and economic evaluation. *Int. J. Ambient Energy* **2018**, *1*, 96–119. [CrossRef]
37. Mutlu, Ö.Ç.; Büchner, D.; Theurich, S.; Zeng, T. Combined Use of Solar and Biomass Energy for Sustainable and Cost-Effective Low-Temperature Drying of Food Processing Residues on Industrial-Scale. *Energies* **2021**, *14*, 561. [CrossRef]
38. Neumann, J.; Jäger, N.; Apfelbacher, A.; Daschner, R.; Binder, S.; Hornung, A. Upgraded biofuel from residue biomass by Thermo-Catalytic Reforming and hydrodeoxygenation. *Biomass Bioenergy* **2016**, *89*, 91–97. [CrossRef]
39. Heindl, A. *Praxisbuch Bandtrocknung: Grundlagen, Anwendung, Berechnung*; Springer: Berlin/Heidelberg, Germany, 2016; ISBN 364253905X.
40. HUBER SE. HUBER Belt Dryer BT for Sewage Sludge Drying. Available online: https://www.huber.de/fileadmin/01_products/04_sludge/04_trocknen/02_bt/pro_bt_en.pdf (accessed on 5 March 2022).
41. Conti, R.; Jäger, N.; Neumann, J.; Apfelbacher, A.; Daschner, R.; Hornung, A. Thermocatalytic Reforming of Biomass Waste Streams. *Energy Technol.* **2016**, *5*, 104–110. [CrossRef]
42. Jäger, N.; Conti, R.; Neumann, J.; Apfelbacher, A.; Daschner, R.; Binder, S.; Hornung, A. Thermo-Catalytic Reforming of Woody Biomass. *Energy Fuels* **2016**, *30*, 7923–7929. [CrossRef]
43. Yang, Y.; Wang, J.; Chong, K.; Bridgwater, A.V. A techno-economic analysis of energy recovery from organic fraction of municipal solid waste (MSW) by an integrated intermediate pyrolysis and combined heat and power (CHP) plant. *Energy Convers. Manag.* **2018**, *174*, 406–416. [CrossRef]
44. Peters, M.S.; Timmerhaus, K.D.; West, R.E. *Plant Design and Economics for Chemical Engineers*, 5th ed.; McGraw-Hill: Boston, MA, USA, 2003; ISBN 0072392665.
45. Green, D.W.; Perry, R.H. *Perry's Chemical Engineers' Handbook*; McGraw-Hill Education: Boston, MA, USA, 2008; ISBN 0071422943.
46. Seider, W.D. *Product and Process Design Principles: Synthesis, Analysis and Evaluation*, 3rd ed.; Wiley: Hoboken, NJ, USA, 2009; ISBN 9780470048955.
47. Chauvel, A.; Fournier, G.; Raimbault, C. *Manual of Process Economic Evaluation*; Editions Technip: Paris, France, 2003; ISBN 2710808366.
48. Brammer, J.G. *Study of Biomass Gasifier-Engine Systems with Integrated Feed Drying for Power and CHP*; Aston University: Birmingham, UK, 2001.
49. Damodaran, A. *Country Risk: Determinants, Measures and Implications*, 2021 ed.; Stern School of Business: New York, NY, USA, 2021.
50. Damodaran, A. *Country Default Spreads and Risk Premiums*; Stern School of Business: New York, NY, USA, 2019.
51. Raza, M.; Inayat, A.; Ahmed, A.; Jamil, F.; Ghenai, C.; Naqvi, S.R.; Shanableh, A.; Ayoub, M.; Waris, A.; Park, Y.-K. Progress of the Pyrolyzer Reactors and Advanced Technologies for Biomass Pyrolysis Processing. *Sustainability* **2021**, *13*, 11061. [CrossRef]
52. Jahangiri, H.; Santos, J.; Hornung, A.; Ouadi, M. Thermochemical Conversion of Biomass and Upgrading of Bio-Products to Produce Fuels and Chemicals. In *Catalysis for Clean Energy and Environmental Sustainability: Biomass Conversion and Green Chemistry—Volume 1*, 1st ed.; Pant, K.K., Gupta, S.K., Ahmad, E., Eds.; Springer: Cham, Switzerland, 2021; pp. 1–47, ISBN 978-3-030-65016-2.
53. Bashir, M.A.; Jahangiri, H.; Hornung, A.; Ouadi, M. Deoxygenation of Bio-oil from Calcium-Rich Paper-Mill Waste. *Chem. Eng. Technol.* **2021**, *44*, 194–202. [CrossRef]
54. del Pozo, C.; Bartrolí, J.; Alier, S.; Puy, N.; Fàbregas, E. Production, identification, and quantification of antioxidants from torrefaction and pyrolysis of grape pomace. *Fuel Process. Technol.* **2021**, *211*, 106602. [CrossRef]
55. Bouaik, H.; Tabal, A.; Barakat, A.; El Harfi, K.; Aboulkas, A. Optimal parameters and structural composition of bio-oil and biochar from intermediate pyrolysis of red algal biomass. *Comptes Rendus. Chim.* **2021**, *24*, 85–99. [CrossRef]
56. Morgano, M.T.; Bergfeldt, B.; Leibold, H.; Richter, F.; Stapf, D. Intermediate Pyrolysis of Agricultural Waste: A Decentral Approach towards Circular Economy. *Chem. Eng. Trans.* **2018**, *65*, 649–654.
57. Molina, A.; Falvey, M.; Rondanelli, R. A solar radiation database for Chile. *Sci. Rep.* **2017**, *7*, 14823. [CrossRef]
58. EIA. Annual Energy Outlook 2021. 2021. Available online: https://www.eia.gov/outlooks/aeo/ (accessed on 5 March 2022).
59. Ben Othman, F.; Eddhibi, F.; Bel Hadj Ali, A.; Fadhel, A.; Guizani, A.; Balghouthi, M. Study of a solar installation for olive mill sludge treatment. *Chem. Eng. Process.-Process Intensif.* **2022**, *172*, 108776. [CrossRef]